Cell. Mol. Life Sci. 66 (2009) 697 – 710
1420-682X/09/040697-14
DOI 10.1007/s00018-009-8652-2
© Birkhäuser Verlag, Basel, 2009

Cellular and Molecular Life Sciences

Research Article

CD20-related signaling pathway is differently activated in normal and dystrophic circulating CD133$^+$ stem cells

D. Parolini[a], M. Meregalli[a], M. Belicchi[a], P. Razini[a], R. Lopa[c], B. Del Carlo[d], A. Farini[a], S. Maciotta[a], N. Bresolin[a], L. Porretti[c], M. Pellegrino[d] and Y. Torrente[a,b,*]

[a] Stem Cell Laboratory, Department of Neurological Sciences, Fondazione IRCCS Ospedale Maggiore Policlinico, Centro Dino Ferrari, University of Milan, via F. Sforza 35, 20122 Milan (Italy), Fax: 0039-02-50320430, e-mail: yvan.torrente@unimi.it
[b] UNISTEM, Centro Interdipartimentale di Ricerca sulle Cellule Staminali, University of Milan, via Balzaretti 9, 20133 Milan (Italy)
[c] Centro Interdipartimentale di Citometria, Department of Regenerative Medicine, Fondazione IRCCS Ospedale Maggiore Policlinico, via F. Sforza 35, 20122 Milan (Italy)
[d] Department of Human Physiology, University of Pisa, via S. Zeno 31, 56127 Pisa (Italy)

Received 15 October 2008; received after revision 27 November 2008; accepted 05 December 2008
Online First 20 January 2009

Abstract. Among the heterogeneous population of circulating hematopoietic and endothelial progenitors, we identified a subpopulation of CD133$^+$ cells displaying myogenic properties. Unexpectedly, we observed the expression of the B-cell marker CD20 in blood-derived CD133$^+$ stem cells. The CD20 antigen plays a role in the modulation of intracellular calcium homeostasis through signaling pathways activation. Several observations suggest that an increase in intracellular calcium concentration ($[Ca^{2+}]_i$) could be involved in the etiology of the Duchenne muscular dystrophy (DMD). Here, we show that a CD20-related signaling pathway able to induce an increase in $[Ca^{2+}]_i$ is differently activated after brain derived neurotrophic factor (BDNF) stimulation of normal and dystrophic blood-derived CD133$^+$ stem cells, supporting the assumption of a "CD20-related calcium impairment" affecting dystrophic cells. Presented findings represent the starting point toward the expansion of knowledge on pathways involved in the pathology of DMD and in the behavior of dystrophic blood-derived CD133$^+$ stem cells.

Keywords. Circulating stem cells, CD133, CD20, Ca^{2+}, Duchenne muscular dystrophy (DMD), brain derived neurotrophic factor (BDNF).

Introduction

Intracellular calcium is an essential regulator of cell function [1–3]. Different mechanisms involved in the precise control of cytosolic concentration of free calcium ($[Ca^{2+}]_i$) were described, including the inositol 1,4,5-trisphosphate (IP_3) cascade and the store-operated calcium (SOC) entries. In particular, the IP_3 production leads to rapid release of Ca^{2+} from intracellular stores in the endoplasmic reticulum. Store depletion activates Ca^{2+} influx across the plasma membrane through the SOC channels, replenishing empty stores and providing a sustained increase in the $[Ca^{2+}]_i$.

* Corresponding author.

Recently, these mechanisms were shown to play a role in skeletal muscle and to be involved in the etiology of muscle fiber injury, especially in some muscular dystrophies, e.g. in Duchenne muscular dystrophy (DMD). DMD is a progressive neuromuscular disease characterized by lack of dystrophin, a 427-kD protein expressed at the inner face of the sarcolemma [4, 5]. In normal skeletal muscle cells, dystrophin is associated at its carboxy-terminal domain with a complex of transmembrane proteins, called dystrophin-associated-proteins (DAP), that also bind merosin (laminin-2), a component of the extracellular matrix. At its amino-terminal domain, dystrophin binds cytoskeletal F-actin filaments. Dystrophin thus constitutes a link between the cytoskeleton and the extracellular matrix. It is now clear that the alteration of dystrophin expression affects DAPs' targeting to the membrane and causes a disruption of the link between the cytoskeleton and the extracellular matrix. This process has two consequences: (a) the cell membrane is more fragile and can be damaged during eccentric muscle contraction; (b) membrane proteins, especially ion channels, are disregulated. Strong perturbations of calcium handling were observed in DMD muscle fibers [6–8]. Moreover, studies performed on dystrophic muscle cells from *mdx* mice, the animal model of DMD [9], have suggested that a persistent intake of Ca^{2+} activates Ca-sensitive proteolytic and phospholipolytic activities [10, 11] resulting in the degradation of dystrophic muscle tissue. However, the question of global elevation in resting $[Ca^{2+}]_i$ values remains controversial in isolated muscle fibers from *mdx* mice and in cultured *mdx* or DMD myotubes as well [12]. Some papers reported elevation in resting $[Ca^{2+}]_i$ of *mdx* myotubes and myofibers [11, 13–15], while other groups did not confirm this increase in steady-state cytosolic calcium levels [16–19]. These controversial results could be influenced by the different state of differentiation of the muscle cells analyzed. In fact, the global elevation of resting $[Ca^{2+}]_i$ could be dependent on differentiation and activity of muscle cells [20]. While DMD myotubes in primary culture did not develop a significant increase in $[Ca^{2+}]_i$ [19, 21], well differentiated DMD myotubes co-cultured with neurons or neural explants displayed elevated steady-state calcium levels [22]. Importantly, alterations of the sodium permeability were not observed in DMD or *mdx* myoblasts, ruling out a general (non-specific) increase of ionic permeability through membrane wounds and supporting the involvement of specific transmembrane channels and intracellular pathways. In particular, the store-operated calcium channels (SOCCs) seem to be involved in the entries of Ca^{2+} in the dystrophic muscle fibers [23]. Otherwise, another explanation of the increased Ca^{2+} release in dystrophic myotubes could either be related to ryanodine receptors [24] or involve the inositol 1,4,5-trisphosphate receptors. Previous study has shown that basal levels of IP_3 were increased two- to threefold in dystrophic human and murine muscle cell lines as compared to normal muscle cell lines [25], suggesting that phospholipase C (PLC), the enzyme that catalyses IP_3 production, could be over-activated in dystrophin-deficient cells. Finally, in dystrophin-deficient cells where expression of full-length dystrophin was forced by plasmid microinjection, the development of calcium-handling abnormalities was prevented by maintaining the resting $[Ca^{2+}]_i$ at low levels and decreasing global calcium-release amplitudes [26]. Furthermore, mini-dystrophin (which lacks 17 repeats of the central rod domain) retains the ability to negatively regulate store-dependent calcium influx and to restore a normal calcium homeostasis. The domains involved in the negative control of SOCCs may be situated in the C-terminal domain, a protein region present in all dystrophin isoforms, included Dp71, and where binding sites for dystrobrevins and syntrophins can be found.

The conditions of calcium-release and the role of SOCCs in dystrophic myogenic progenitors are not known. We previously described the myogenic capacity of human blood-derived progenitors expressing the CD133 surface marker [27, 28]. The extensively described impairment of Ca^{2+} homeostasis affecting dystrophic muscular cells, together with its central role in all living cells physiology, prompted us to focus our efforts on the evaluation of calcium handling in normal and dystrophic blood-derived CD133$^+$ stem cells and, eventually, on the molecular characterization of highlighted differences.

In this work we demonstrate that dystrophic circulating CD133$^+$ stem cells display an impaired calcium homeostasis related to brain derived neurotrophic factor (BDNF) overproduction and CD20 signaling pathway, suggesting the importance of a normal dystrophin-based cytoskeleton in the maintenance of a correct intracellular Ca^{2+} homeostasis.

Materials and methods

RT-PCR and Western blotting for the evaluation of dystrophin isoforms expression. Total RNA was extracted from normal and dystrophic circulating CD133$^+$ stem cells by TrizolReagent (Invitrogen, Carlsbad, CA, USA). First-strand cDNA was prepared by using Super Script First Strand Synthesis System for RT-PCR (Invitrogen, Carlsbad, CA, USA), starting from 2 μg total RNA with oligo$(dT)_{12-18}$ primers. To investigate the expression

of the most common dystrophin isoforms, we designed five different pairs of human-specific primers: dys-427 kD F(5'-CCTACAGGACTCAGATCTGG-3') and R(5'-GTCCTCTACTTCTTCCCACC-3'); dys-260 kD F(5'-GCATCCAGTCTGCCCAGG-3') and R(5'-GAGACAGGACTCTTTGGGCAG-3'); dys-140 kD F(5'-GGATGGCATTGGGCAGCG-3') and R(5'-GCTCTTTTCCAGGTTCAAGTGG-3'); dys-116 kD F(5'-CCTCCAAGGTGAAATT-GAAGC-3') and R(5'-CTGGCTTCCAAATGG-GACC-3'); dys-71 kD F(5'-CCACGAGACTCA-AACAACTTGC-3') and R(5'-CTTGAGGTTGT-GCTGGTCC-3'). The GAPDH gene was amplified as a standard using the following couple of primers: F(5'-GCACAAGAGGAAGAGAGAGAC-3') and R(5'-GATGGTACATGACAAGGTGCGG-3').

PCR was performed on cDNA samples obtained from blood-derived $CD133^+$ stem cells cultured in proliferative conditions, and PCR products were analyzed on 2 % agarose gels.

For Western blot analysis of Dp71, normal and dystrophic circulating $CD133^+$ stem cells and $CD133^-$ cells were lysed directly in 1X sample buffer (1 % SDS) containing 2 μg/ml aprotinin, 10 μg/ml leupeptin, 10 mM sodium fluoride (NaF), 1 mM sodium vanadate (Na_3VO_4) and 1 mM phenylmethylsulfonylfluoride (PMSF). Lysates were boiled 5 min and centrifuged at 10 000 x g for 5 min to remove insoluble material. Total protein concentration was determined according to Lowry's method [29] and lysates were stored at -20 °C. Samples were analyzed on 7.5 % polyacrylamide gel, transferred to supported nitrocellulose membranes (Bio-Rad Laboratories, Hercules, CA, USA), and the filters were saturated in blocking solution (10 mM Tris, pH 7.4, 154 mM NaCl, 1 % BSA, 10 % horse serum, 0.075 % Tween-20) overnight at 4 °C. Primary antibodies (NCL-Dys2 – Novocastra Laboratories, Newcastle, UK; anti-β-actin – Sigma, Milan, Italy) were incubated for 90 min at room temperature and then followed by washing, detection with horseradish peroxidase (HRP) conjugated secondary antibodies (DakoCytomation, Carpinteria, CA, USA), and developed by enhanced chemiluminescence (ECL) (Amersham Biosciences, Piscataway, NJ, USA). Prestained molecular weight markers (Bio-Rad Laboratories, Hercules, CA, USA) were run on each gel. Bands were visualized by autoradiography using Amersham Hyperfilm™ (Amersham Biosciences, Piscataway, NJ, USA).

Isolation and characterization of blood-derived $CD133^+$ stem cell fraction for FACS analysis. Circulating $CD133^+$ stem cells were collected from peripheral blood of normal subjects and DMD patients, after informed consent was obtained, according to the guidelines of the Committee on the Use of Human Subjects in Research of the Policlinico Hospital of Milan (Milan, Italy). The protocol of cell isolation was previously described [28]. After determination of the purity of the $CD133^+$ stem cells, we plated the cells in the presence of a proliferation medium (PM) composed of DMEM/F-12 (1:1); 20 % FBS, including Hepes (N-(2-hydroxyethyl)piperazine-N'-(ethanesulfonic acid)) buffer (5 mM), glucose (0.6 %), sodium bicarbonate (3 mM), and glutamine (2 mM); SCF (100 ng/ml; TEBU, Frankfurt, Germany); VEGF (50 ng/ml; TEBU, Frankfurt, Germany); and LIF (20 ng/ml; R&D Systems, Minneapolis, MN, USA). Cell viability assay was performed using 7-Amino-actinomycin D (7-AAD) viability probe. For four-color flow cytometric analysis, at least 30 x 10^4 to 80 x 10^4 cells were incubated with the following monoclonal antibodies (mAbs): anti-CD133/2-phycoerythrin (PE) (Miltenyi Biotec, Germany), anti-CD34-Allophycocyanin (APC) (BD, Franklin Lakes, NJ, USA), anti-CDw90 (Thy-1)-fluorescein-isothiocyanate (FITC) (BD, Franklin Lakes, NJ, USA), anti-VEGF-R2 (KDR)-PE (R&D Systems, Minneapolis, MN, USA), anti-CD184 (CXCR4, fusin)-PE-Cy5 (BD, Franklin Lakes, NJ, USA), anti-CD45-FITC (BD, Franklin Lakes, NJ, USA), and anti-CD20-FITC (BD, Franklin Lakes, NJ, USA). For each mAb, an appropriate isotype-matched mouse immunoglobulin was used as a control. After staining performed at 4 °C for 20 min, cell suspensions were washed in PBS containing 1 % heat inactivated FCS and 0.1 % sodiumazide. Cells were analyzed using a FACSCalibur flow cytometer and PAINT-a Gate software (BD, Franklin Lakes, NJ, USA). The commercially available BDKit (BD, Franklin Lakes, NJ, USA) was used to quantify the number of $CD20^+$ cells among normal and dystrophic circulating $CD133^+$ stem cells. The commercially available Quantibrite™ Beads system (BD, Franklin Lakes, NJ, USA) was used to determine the number of CD20 molecules on membrane of normal and dystrophic circulating $CD133^+$ stem cells, according to manufacturer's instructions.

Immunoprecipitation and Western immunoblotting. For the precipitation of CD20 complexes, cells were pelletted at 3000 rpm for 7 min at 4 °C and then lysed in 1 % Nonidet P-40 detergent buffer containing 20 mM Tris, pH 8, 137 mM NaCl, 2 mM EDTA, 10 % glycerol, 2 μg/ml aprotinin, 10 μg/ml leupeptin, 10 mM NaF, 1 mM Na_3VO_4 and 1 mM PMSF. After 15 min on ice with occasional agitation, samples were centrifuged at 10000 x g for 10 min at 4 °C to remove insoluble material. Total protein concentration was determined according to Lowry's method [29] and

lysates were stored at -20 °C. Lysates (200–300 μg of total proteins) were incubated with 10 μg of anti-CD20 antibody (M-20, Santa Cruz Biotechnology, Inc., Santa Cruz, CA, USA) and mixed overnight at 4 °C before adding 50 μl of Protein A/G PLUS-Agarose (Santa Cruz Biotechnology, Inc., Santa Cruz, CA, USA). Beads were incubated for 3 h at 4 °C and then washed 3 times with PBS before addition of 30 μl of 1X sample buffer containing 1% SDS. Samples were boiled for 5 min, centrifuged at 10000 x g for 5 min at room temperature and supernatants (IP samples) were resolved on 10% polyacrylamide gels. After transfer to supported nitrocellulose membranes (Bio-Rad Laboratories, Hercules, CA, USA), the filters were saturated in blocking solution (10 mM Tris, pH 7.4, 154 mM NaCl, 1% BSA, 10% horse serum, 0.075% Tween-20) overnight at 4 °C, incubated with primary antibodies, and then followed by washing, detection with HRP-conjugated secondary antibodies (DakoCytomation, Carpinteria, CA, USA), and developed by ECL (Amersham Biosciences, Piscataway, NJ, USA). Prestained molecular weight markers (Bio-Rad Laboratories, Hercules, CA, USA) were run on each gel. Bands were visualized by autoradiography using Amersham Hyperfilm™ (Amersham Biosciences, Piscataway, NJ, USA). CD20 phopshorylation state was investigated using anti-phosphothreonine (H-2, Santa Cruz Biotechnology, Inc., Santa Cruz, CA, USA) and anti-phosphoserine (16B4, Santa Cruz Biotechnology, Inc., Santa Cruz, CA, USA) primary antibodies. For the evaluation of Lyn recruitment to CD20 and activation, filters were incubated with specific anti-Lyn antibody (#2732, Cell Signaling Technology, Inc., Danvers, MA, USA), then stripped and reprobed with anti-phosphotyrosine antibody (PY99, Santa Cruz Biotechnology, Inc., Santa Cruz, CA, USA). Obtained bands were acquired using the Epson Perfection 2400 PHOTO Scanner and the Epson Scan Software. Densitometric analysis were performed using ImageJ software (http://rsbweb.nih.-gov/ij/).

Measurement of cytoplasmic calcium concentration $[Ca^{2+}]_i$. Cells were suspended in a physiological solution (PS) containing NaCl 154 mM, KCl 5 mM, $MgCl_2$ 1 mM, $CaCl_2$ 1.8 mM, Glucose 10 mM, Hepes 10 mM (pH adjusted to 7.4 with NaOH) and centrifuged for 4 min at 1500 x g. Cells were loaded with Ca^{2+} indicators by incubation in the PS solution containing the acetoxy methyl ester (AM) of Fura-2 (9 μM in dimethyl sulfoxide [DMSO]) or Fluo3 (2 μM in DMSO) (Molecular Probes Europe, Leiden, The Netherlands), for 45 min at room temperature (20–22 °C), in the dark, with gentle mixing. Cells were then centrifuged, resuspended in PS and allowed to complete hydrolysis of AM ester groups for 30 min at room temperature. Images were obtained with a fluorescence microscope (Nikon Eclipse 600), using a CFI Fluor 60X, 1.0 NA, water-immersion objective. Cells were settled, at low density, in a glass imaging chamber. Images were acquired by a CCD camera (Panasonic, WV-BP514E) and collected using Axon Imaging Workbench 2.2 software (Axon Instruments Inc., CA, USA), by averaging 16 frames (time of exposure 528 ms). To visualize changes of $[Ca^{2+}]_i$ Fluo3 loaded cells were imaged at 520 nm by exciting at 480 nm every 5–30 s to minimize dye photobleaching. The fluorescence signals, F_{base} and F, were computed as the mean pixel value in each region of interest covering a single cell, at the beginning and during the time course, respectively. The normalized change in fluorescence was reported as a pseudoratio, which is thought to approximately reflect $[Ca^{2+}]_i$ and was calculated using the equation: $\Delta F/F = (F\text{-}F_{base})/(F_{base}\text{-}B)$, where B is the background signal averaged over cell free areas. To measure the intracellular free Ca^{2+} levels, Fura-2 loaded cells were alternatively excited at 340 and 380 nm while they were imaged at 510 nm at room temperature. After background subtraction, ratio images were obtained by dividing pixel by pixel couples of digitized images at 340 and 380 nm. In each cell the fluorescence intensity was measured by the mean pixel value in a region of interest covering most of the cell area. Fluorescence values can be converted into ion concentrations according to the equation given by Grynkiewicz and colleagues [30]: $[Ca^{2+}] = K_d\ [(R\text{-}R_{min})/(R_{max}\text{-}R)]\ X\ (F_{f380}/F_{b380})$, where R is the ratio of the fluorescence intensities measured at 340 and 380 nm, R_{min} is the limiting value of R when all the indicator is in the Ca^{2+}-free form, R_{max} when it is saturated with calcium, K_d is the dissociation constant of the Fura-2-calcium complex, F_{f380} and F_{b380} are the fluorescence intensities of Ca^{2+}- free and Ca^{2+}- bound Fura-2 at 380 nm, respectively. For calibration, Ca^{2+}- saturated or Ca^{2+}-free dye can be set by 5 μM ionomycin in the presence of 2.5 mM Ca^{2+} or by 10 mM EGTA (ethyleneglycol-bis(ß-aminoethyl ether)N,N-tetraacetic acid) in nominally Ca^{2+}-free solution, respectively. Ionomycin was purchased from Calbiochem (Inalco, Italy) whilst all other reagents were obtained from Sigma (Milan, Italy). We also performed measurements of intracellular calcium on normal and dystrophic circulating CD133$^+$ stem cells after stimulation with 100 ng/ml BDNF in RPMI 1640 medium (Gibco – Invitrogen, Carlsbad, CA, USA). The cells were analyzed 2 h after BDNF stimulation.

Immunoassay of cell culture supernatants. After 24 h of culture, media from normal and DMD blood-

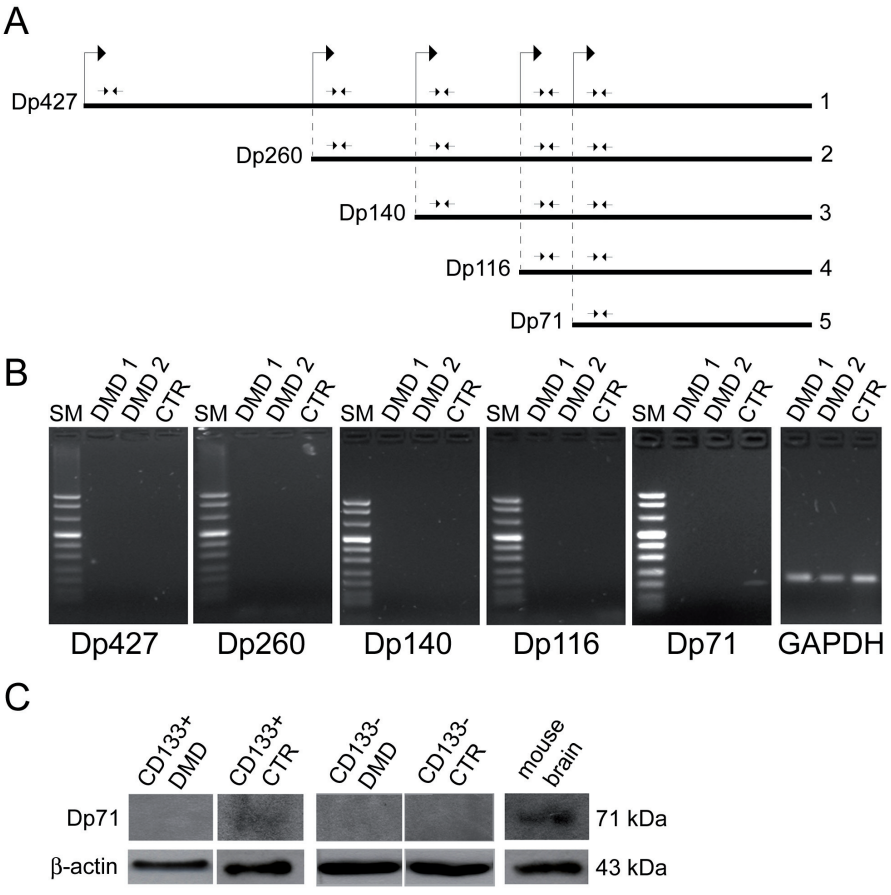

Figure 1. Dp71 expression by circulating CD133$^+$ stem cells. (*A*) Schematic map showing the five major human dystrophin isoforms and the primers used to distinguish the isoforms. (*B*) PCR results from normal and dystrophic blood-derived CD133$^+$ stem cells after seven days of culture in proliferation (stem-cell-conditioned) media. The first five gels correspond to the expression of the different dystrophin isoforms indicated in (*A*). Last gel corresponds to the amplification of the GAPDH gene as standard (PCR fragment 150 bp). Only the Dp71 mRNA is expressed by normal circulating CD133$^+$ stem cells in these conditions (PCR fragment 193 bp). (Size Marker, SM). (*C*) Immunoblotting analysis confirmed that only normal blood-derived CD133$^+$ stem cells are able to express the Dp71 dystrophin isoform also at protein level (lane CD133$^+$ CTR). Neither normal nor dystrophic CD133$^-$ cells expressed the Dp71 at protein level (lanes CD133$^-$ DMD and CD133$^-$ CTR). Mouse brain homogenate was used as control. β-actin immunoblotting indicated that the same protein concentration was present in all specimens.

derived CD133$^+$ stem cells were collected and used for ELISA quantification of secreted cytokines. Quantikine® Immunoassay (R&D Systems, Minneapolis, MN, USA) specific for human IGF-1, VEGF, BDNF and TGFβ-1 were performed according to manufacturer's instructions. Media were added to a 96-well polystyrene microplate coated with specific monoclonal antibodies. Secreted cytokine was detected by treating the plates with the respective polyclonal or monoclonal HRP conjugated detection antibody. Enzyme substrate was added to generate a color product whose absorbance was read at 450 nm. A cytokine standard included in each assay was used to generate a standard curve that was used to calculate the amount of secreted cytokine per well. Samples were assayed in duplicate.

Results

Circulating CD133$^+$ stem cells express the Dp71 dystrophin isoform. Total mRNA was collected and analyzed by RT-PCR. Normal blood-derived CD133$^+$ stem cells expressed the mRNA of the ubiquitous 71-kD dystrophin isoform (Fig. 1 B). No expression of the 116-kD, 140-kD, 260-kD and 427-kD dystrophin isoforms mRNA was observed in these cells (Fig. 1 B). On the contrary, although the DMD genotypes analyzed (Δ11–13; Δ26–30; Δ45–52; Δ4-6-8-12-13; Δ17–44; Δ42–51; Δ43–45; Δ49–52; exon 2 duplication) were formally compatible with the expression of Dp71, all the dystrophin isoforms mRNA were absent in dystrophic circulating CD133$^+$ stem cells, including the Dp71 (Fig. 1 B). As expected, the Western blot analysis confirmed the expression of the Dp71 dystrophin isoform only in the normal blood-derived CD133$^+$ stem cells (Fig. 1 C). Importantly, neither normal nor dystrophic circulating CD133$^-$ cells expressed the Dp71 dystrophin isoform (Fig. 1 C), demonstrating that the expression of Dp71 is a CD133$^+$ stem cells specific feature.

FACS immunophenotyping of blood-derived CD133$^+$ stem cells. Surface antigens expressed by normal and dystrophic circulating CD133$^+$ stem cells were characterized by means of flow cytometry analysis. Hoechst 33342 staining did not reveal the presence of Side Population (SP) fraction among isolated CD133$^+$ cells (99 % ± 1 % [mean ± SD])(data not shown), moreover up to 98 % of blood-derived

CD133$^+$ stem cells showed a lin$^-$ phenotype (CD4$^-$ CD8$^-$ CD3$^-$ CD19$^-$ CD33$^-$ CD38$^-$) (data not shown). Normal and dystrophic circulating CD133$^+$ stem cells represented less than 0.2 % (range 0.04–0.1 %, n = 12 normal blood; range 0.06–0.2 %, n = 33 DMD blood) of total blood mononucleated cells as previously described [28]. Interestingly, normal and dystrophic circulating CD133$^+$ stem cells co-expressed the B-cell marker CD20 (Fig. 2 A). More than 92 % of normal and dystrophic circulating CD133$^+$CD20$^+$ cells also co-expressed CXCR4 and CD34 antigens (Fig. 2 A). By FACS analysis, the percentage of CD133$^+$ stem cells expressing the CD20 antigen was not statistically significantly higher in the DMD subpopulation than the normal counterpart (27.9 % ± 11 % vs. 30.1 % ± 13.1 %; $p>0.5$) (Fig. 2 A). Moreover, two subpopulations within the circulating CD133$^+$CD20$^+$ cells were observed distinguishing the CD133$^+$CD20^{bright} (1.7 ± 2.1 and 2.1 ± 1.5 cells/μl from normal and dystrophic blood samples, respectively; $p>0.5$) and the CD133$^+$CD20^{dim} (0.8 ± 0.3 vs. 1.1 ± 0.5 cells/μl; from normal and dystrophic blood samples, respectively; $p>0.5$) (Fig. 2 B). In order to quantify the number of CD20 molecules on the circulating CD133$^+$CD20$^+$ cells we used the Quantibrite™ Beads system. By this method we found no significant differences between the number of CD20 antigens expressed in normal and dystrophic CD133$^+$CD20^{bright} (27780 ± 12681 vs. 31419 ± 18112 antibody bound per cell, ABC; $p>0.5$) and CD133$^+$CD20^{dim} (1307 ± 491 vs. 1469 ± 1023 antibody bound per cell, ABC; $p>0.5$) (Fig. 2 C). These results demonstrate that the percentage of circulating CD133$^+$CD20$^+$ cells and the number of CD20 molecules expressed on the cell membrane is similar in normal and dystrophic specimens.

CD20 antigen phosphorylation is enhanced in dystrophic blood-derived CD133$^+$ stem cells. To test whether the unexpected expression of CD20 antigen in the circulating normal and dystrophic CD133$^+$ stem cells could be related to a possible functional pathway, we decided to look at its phosphorylation state by performing immunoprecipitation experiments followed by Western blotting. No tyrosine residues or recognized signaling motifs occur in any of the cytoplasmic regions of CD20, although there are a number of consensus sites for serine or threonine phosphorylation [31]. CD20 was immunoprecipitated from normal and dystrophic circulating CD133$^+$ stem cells, separated by SDS-PAGE, transferred to membranes and probed with anti-phosphoserine or anti-phosphothreonine antibody. No difference was observed concerning serine phosphorylation between normal and dystrophic circulating CD133$^+$ stem cells (data not shown), while CD20 showed a higher threonine phosphorylation in dystrophic circulating CD133$^+$ stem cells (Fig. 2 D). Taken together these observations supported the state of activation of the CD20 antigen, particularly in dystrophic circulating CD133$^+$ stem cells.

Impairment of calcium homeostasis in blood-derived dystrophic CD133$^+$ stem cells. Since the CD20 expression and its phosphorylation state in the circulating CD133$^+$ stem cells could be involved in the regulation of the calcium homeostasis of these cells, we first performed measurements of $[Ca^{2+}]_i$ on normal and dystrophic blood-derived CD133$^+$ stem cells. In these experiments we evaluated the number of cells displaying a concentration of cytosolic free calcium to be higher than a reference value of 100 nM. In order to quantify the intracellular calcium, we used the dual-wavelength ratiometric dye Fura-2. In this experiment we found a significantly higher percentage of cells exceeding this reference value in dystrophic circulating CD133$^+$ stem cells compared to the normal counterpart ($p<0.001$) (Fig. 3 A). We also noted that dystrophic circulating CD133$^+$CD20$^+$ cells displayed a higher susceptibility than their normal counterparts to increase $[Ca^{2+}]_i$ in response to both high $[K]_o$ (100 mM) and ionomycin (1 μM) (Fig. 3 B). This feature was not further studied. However, these data suggest an impairment of Ca^{2+} homeostasis in the circulating dystrophic CD133$^+$CD20$^+$ cells.

Abnormal BDNF release from blood-derived dystrophic CD133$^+$ stem cells. Since no natural agonist for CD20 has been identified until now, we considered the possibility that CD20 channel and/or signal transduction activity can be indirectly activated by cytokines or growth factors after interaction with their own receptors and consequent activation of intracellular signaling cascades. Following this hypothesis, we decided to perform an ELISA screening, looking for released factors over-expressed by dystrophic circulating CD133$^+$ stem cells. Supernatants were collected after 24 h of culture and the concentrations of IGF-1, VEGF, BDNF and TGFβ-1 were measured. Results are expressed as a ratio concentration/cell number in culture. While IGF-1 and VEGF were detected in similar amounts in normal and dystrophic circulating CD133$^+$ stem cell supernatants (IGF-1: 1.1×10^{-7} normal vs. 1.8×10^{-7} dystrophic) (Fig. 4 A); (VEGF: 2.0×10^{-3} normal vs. -8.5×10^{-4} dystrophic) (Fig. 4 B), BDNF and TGFβ-1 displayed a different release profile comparing healthy and dystrophic circulating CD133$^+$ stem cells. BDNF measurement in dystrophic blood-derived CD133$^+$ stem cell supernatant returned a ratio that was six-fold increased in comparison to that

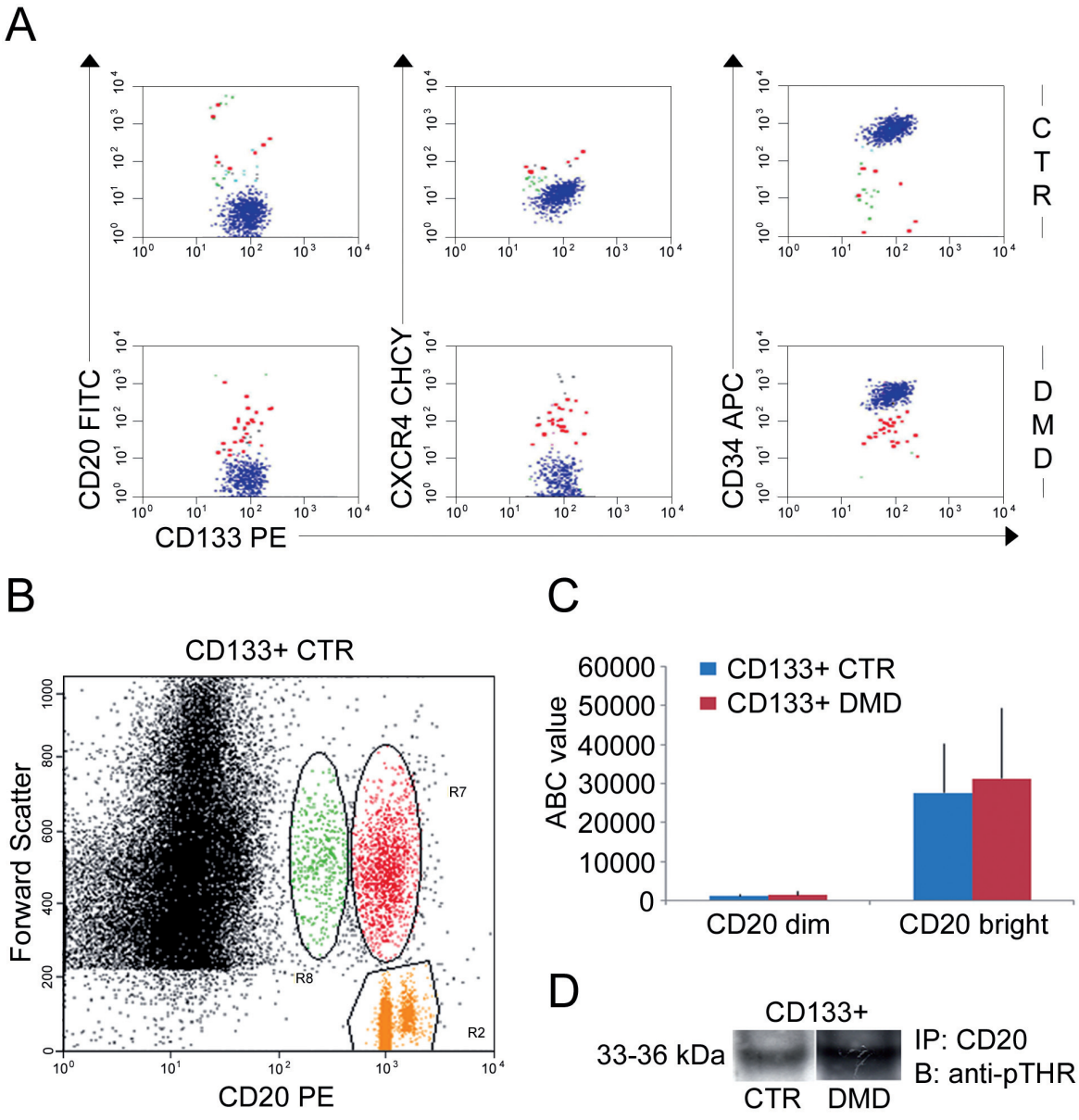

Figure 2. Characterization of blood-derived CD133$^+$ stem cells immunophenotype. (*A*) FACS immunophenotyping of the fractionated normal (lane CTR) and dystrophic (lane DMD) circulating CD133$^+$ stem cells. Normal and dystrophic circulating CD133$^+$ stem cells co-expressed the B-cell marker CD20 (27.9 % ± 11 % normal vs. 30.1 % ± 13.1 % dystrophic; p>0.5), and more than 92 % of normal and dystrophic circulating CD133$^+$CD20$^+$ cells also co-expressed CXCR4 and CD34 antigens. (*B*) The BDKit analysis allowed us to identify two subpopulations within the circulating CD133$^+$ stem cells distinguishing the CD133$^+$CD20^{bright} (1.7 ± 2.1 and 2.1 ± 1.5 cells/µl from normal and dystrophic blood samples respectively; p>0.5) and the CD133$^+$CD20^{dim} (0.8 ± 0.3 vs. 1.1 ± 0.5 cells/µl; from normal and dystrophic blood samples respectively; p>0.5). (*C*) The BD Quantibrite™ Beads system was used to quantify the number of CD20 molecules on the circulating CD133$^+$CD20$^+$ cells. No significant differences were found in the number of CD20 antigens expressed by normal and dystrophic CD133$^+$CD20^{bright} (27780 ± 12681 vs. 31419 ± 18112 antibody bound per cell, ABC; p>0.5) and CD133$^+$CD20^{dim} (1307 ± 491 vs. 1469 ± 1023 antibody bound per cell, ABC; p>0.5). (*D*) Immunoblotting results showed an increased phosphorylation of CD20 on threonine residues in dystrophic circulating CD133$^+$ stem cells (lane DMD) in comparison to the normal counterpart (lane CTR).

obtained from normal cells (1.5×10^{-4} normal vs. 6.1×10^{-4} dystrophic; $p<0.05$) (Fig.4 C). A similar trend was observed considering TGF-β1, with a ratio of 5.8×10^{-3} in normal circulating CD133$^+$ stem cells that increased to a value of 2.6×10^{-2} in dystrophic circulating CD133$^+$ stem cells ($p<0.05$, Fig. 4 D). In order to verify whether the increased ratio obtained after BDNF and TGFβ-1 dosage in DMD supernatants was a CD133$^+$ stem cells specific feature, we performed the same measurements on normal and dystrophic CD133$^-$ cells. Even with no significant difference, TGFβ-1 ratio showed the same increasing

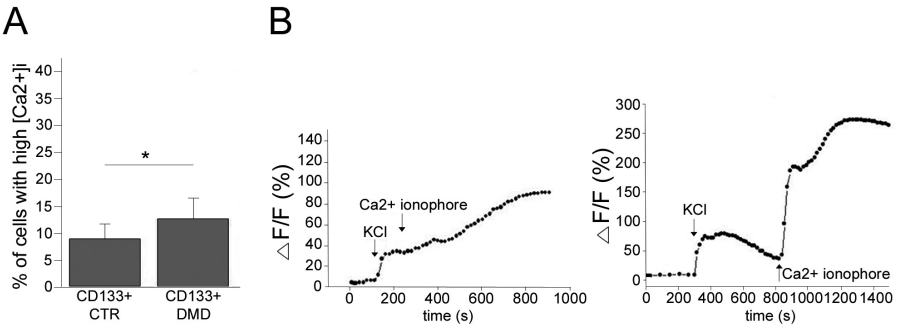

Figure 3. Evaluation of intracellular free Ca^{2+} levels in normal and DMD blood-derived $CD133^+$ stem cells. The dual-wavelength ratiometric dye Fura-2 was used to acquire quantitative intracellular calcium measurements in normal and dystrophic circulating $CD133^+$ stem cells. A reference concentration of 100 nM (in resting cells) was taken as the cut off value to identify cells with high $[Ca^{2+}]_i$. (*A*) The number of normal and dystrophic blood-derived $CD133^+$ stem cells displaying an $[Ca^{2+}]_i$ exceeding the reference value of 100 nM was quantified and expressed as percentage (%) of the total cells analyzed. The number of cells with high $[Ca^{2+}]_i$ was significantly higher in DMD blood-derived $CD133^+$ stem cells than in normal counterpart ($p<0.001$). (*B*) Illustrates the time course of the change in the Fluo3 emission in normal (left side) and dystrophic (right side) circulating $CD133^+CD20^+$ cells, induced by raising the extracellular KCl concentration from 5 to 100 mM and then applying calcium ionophore during the early response steady state. $[Ca^{2+}]_i$ increase, measured as pseudoratio ($\Delta F/F\%$), was abnormally high in dystrophic circulating $CD133^+CD20^+$ cells.

trend observed in dystrophic circulating $CD133^+$ stem cells (Fig. 4 F). On the contrary, the ratio obtained after BDNF dosage was similar comparing normal and dystrophic $CD133^-$ cells (Fig. 4 E). Reported data clearly describe two different phenomena: 1) a generalized TGFβ-1 over-expression affecting dystrophic circulating cells, with no difference between CD133 positive and negative fractions; 2) a BDNF over-expression that specifically affects dystrophic circulating $CD133^+$ stem cells, thus promoting this cytokine as a possible candidate for the indirect modulation of CD20 phosphorylation and signaling activity.

BDNF induces CD20-related intracellular signaling activation in dystrophic blood-derived $CD133^+$ stem cells. Since all the functions of BDNF are mediated by the TrkB pathway, including the protein kinase C (PKC), an enzyme involved in CD20 phosphorylation [32–35], we investigated the role of BDNF in CD20 phosphorylation and signaling modulation. We first decided to evaluate the effect of BDNF on CD20 phosphorylation performing immunoprecipitation and Western blotting experiments. Normal and dystrophic circulating $CD133^+$ stem cells were stimulated with BDNF (100 ng/ml for 2 h) and CD20 immunoprecipitation was performed on cell lysates followed by phosphothreonine immunoblotting. After BDNF treatment, a strong induction of CD20 phosphorylation was observed both in normal and dystrophic blood-derived $CD133^+$ stem cells (Fig. 5 A). Moreover, in dystrophic circulating $CD133^+$ stem cells CD20 was heavily threonine-phosphorylated also in basal condition, probably as a consequence of the higher BDNF release described above (Fig. 5 A). Tyrosine kinases can associate with the cytoplasmic regions of cell-surface molecules by different mechanisms, promoting intracellular signaling transduction. Previous studies reported CD20-specific association with src-family members Lyn, Fyn and Lck, along with a tyrosine phosphorylated protein (p75/80) later identified as PAG, a ubiquitous adaptor protein [31, 36, 37]. Importantly, it is possible that changes in either the conformation of CD20 or its phosphorylation state, or both, could regulate its association with such kinases. To determine whether or not BDNF-induced phosphorylation is followed by the activation of CD20-related downstream signaling pathway, we performed experiments in order to analyze CD20-recruited src kinases and their activation state. Considering that Lyn accounted for most of the protein tyrosine kinase (PTK) activity in the CD20 complex [36], we focused our attention on this src-family member. Immune complexes were prepared from lysates of normal and dystrophic circulating $CD133^+$ stem cells using anti-CD20 antibody. After SDS-PAGE separation, membranes were blotted with anti-Lyn antibody, then stripped and re-probed for the evaluation of tyrosine phopshorylation. Densitometric analysis performed on obtained bands showed that, although Lyn was co-immunoprecipitated with CD20 in all the conditions tested, after BDNF stimulation CD20 immune complexes contained a higher Lyn content both in normal and dystrophic circulating $CD133^+$ stem cells, suggesting an induction of Lyn-CD20 interaction after BDNF exposure (Fig. 5 B). Particularly, even if CD20-recruited Lyn was higher in dystrophic unstimulated blood-derived $CD133^+$ stem cells in comparison to normal unstimulated blood-derived $CD133^+$ stem cells (threefold increase), the

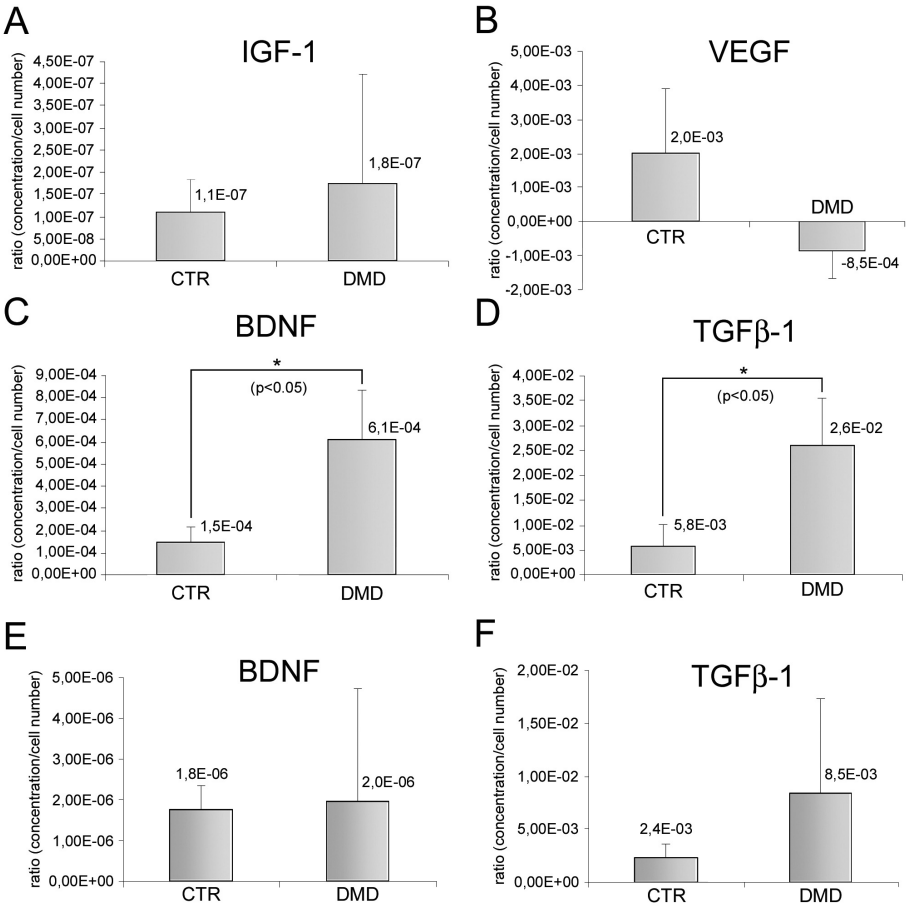

Figure 4. ELISA quantification of cytokines release by normal and DMD blood-derived CD133$^+$ stem cells. Cytokine production by normal and dystrophic circulating CD133$^+$ stem cells was assayed by ELISA method. Supernatants were collected after 24 h of culture and the concentrations of IGF-1, VEGF, BDNF and TGFβ-1 were measured. Results are expressed as a ratio concentration/cell number in culture. While IGF-1 and VEGF were detected in similar amount in normal and dystrophic circulating CD133$^+$ stem cell supernatants (*A* and *B*), BDNF measurement in dystrophic blood-derived CD133$^+$ stem cell supernatant returned a ratio that was six-fold increased in comparison to that obtained from normal cells (*C*). A similar trend was observed considering TGF-β1 (*D*). Measurements performed on normal and dystrophic CD133$^-$ cell supernatants (*E* and *F*) allowed us to identify BDNF over-expression as an exclusive property of dystrophic circulating CD133$^+$ stem cells, while TGFβ-1 over-expression affects dystrophic circulating cells with no difference between CD133 positive and negative fractions.

effects promoted by BDNF on Lyn association to CD20 were more consistent in dystrophic circulating CD133$^+$ stem cells (+43 %) than in normal circulating CD133$^+$ stem cells (+30 %) (Fig. 5 C). Membrane reprobing with anti-phosphotyrosine antibody allowed us to analyze the activation state of CD20-recruited Lyn. After BDNF treatment, only dystrophic circulating CD133$^+$ stem cells showed phosphorylation increase in the Lyn fraction co-immunoprecipitated with CD20 (Fig. 5 D). As a consequence, the ratio phopsho/total protein decreased differently in normal (–29 %) and dystrophic circulating CD133$^+$ stem cells (–9 %) (Fig. 5 E). Together, these results demonstrate that CD20-related signaling can be indirectly modulated by BDNF. Interestingly, effects on CD20 threonine phosphorylation and Lyn recruitment were observed, even if with different intensity, both in normal and dystrophic circulating CD133$^+$ stem cells. On the contrary, only in dystrophic blood-derived CD133$^+$ stem cells does recruited Lyn undergo phosphorylation after BDNF treatment, possibly promoting the activation of additional intracellular pathways that can act synergically with TrkB.

BDNF induces a different increase of intracellular free Ca^{2+} levels in normal and dystrophic circulating CD133$^+$ stem cells. Differences concerning the activation of CD20-recruited Lyn after BDNF stimulation, observed while comparing normal and dystrophic circulating CD133$^+$ stem cells, invited us to consider the effects on cytosolic Ca^{2+} promoted by a potential simultaneous activation of TrkB and CD20-Lyn pathways in dystrophic circulating CD133$^+$ stem cells. As previously described, once activated, TrkB can drive intracellular Ca^{2+} release by means of PLCγ activation and consequent production of the second messenger IP_3. Lyn activation triggers a cascade of signaling events mediated by Lyn phosphorylation of tyrosine residues within the immunoreceptor tyrosine-based activation motifs of receptor proteins, and subsequent recruitment and activation of other kinases, PLCγ2 and phosphoinositide 3-kinase (PI3-K) [38]. These kinases provide activation signals that play critical roles in proliferation, cell differentiation and Ca^{2+} mobilization. Since in normal cells Lyn is recruited by CD20 but fails to become phosphorylated, the synergic action between the two pathways after BDNF exposure could take place only in dystrophic circulating CD133$^+$ stem cells, where a

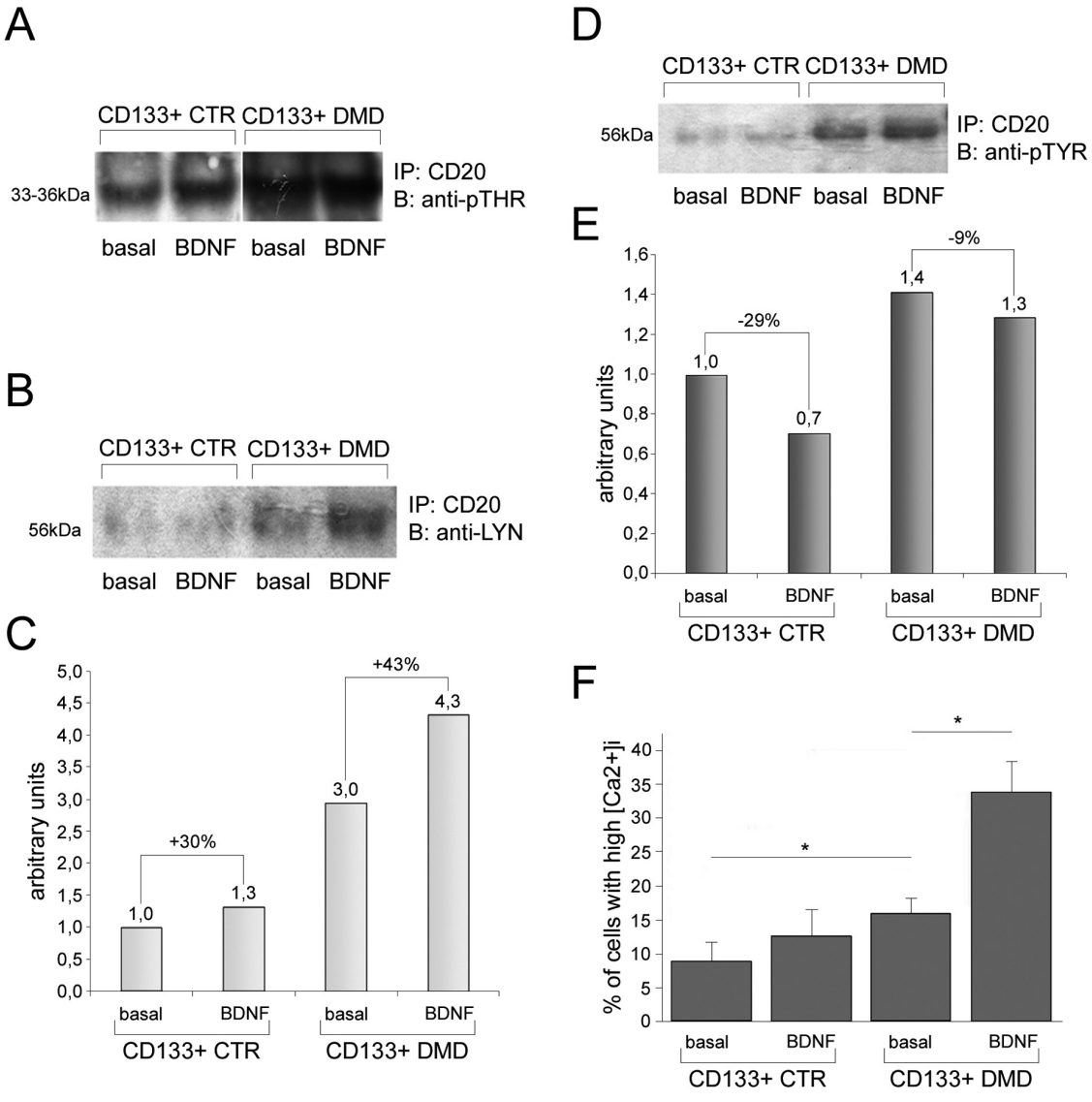

Figure 5. BDNF modulation of CD20-related signaling pathway. (*A*) The role of BDNF in the modulation of CD20-related pathway was first assayed analyzing CD20 antigen phosphorylation in response to BDNF exposure. After BDNF treatment, a strong induction of CD20 phosphorylation was observed both in normal and dystrophic blood-derived $CD133^+$ stem cells (lanes BDNF) in comparison to unstimulated cells (lanes basal). In dystrophic circulating $CD133^+$ stem cells CD20 was heavily threonine-phosphorylated also in basal condition, probably as a consequence of the higher BDNF release described. (*B*) To test whether or not BDNF-induced phosphorylation is followed by activation of the CD20-related downstream signaling pathway, we performed experiments in order to analyze CD20-recruitement of the src-family kinase Lyn. After BDNF stimulation CD20 immune complexes contained a higher Lyn content both in normal and dystrophic circulating $CD133^+$ stem cells, suggesting an induction of Lyn-CD20 interaction after BDNF exposure. (*C*) Densitometric analysis showed a threefold increase in the CD20-recruited Lyn in dystrophic unstimulated blood-derived $CD133^+$ stem cells in comparison to the normal unstimulated blood-derived $CD133^+$ stem cells. Despite that, the effects promoted by BDNF on Lyn association to CD20 were more consistent in dystrophic circulating $CD133^+$ (+43%) than in normal circulating $CD133^+$ (+30%). (D) In order to analyze the activation state of CD20-recruited Lyn, the membranes blotted with anti-Lyn antibody were stripped and re-probed for the evaluation of tyrosine phopshorylation. After BDNF treatment only dystrophic circulating $CD133^+$ stem cells showed a phosphorylation increase in the Lyn fraction co-immunoprecipitated with CD20. (*E*) As a consequence of that which is explained in (*D*) the ratio phopsho/total protein decreased differently in normal (–29%) and dystrophic circulating $CD133^+$ stem cells (–9%). (*F*) To assess the hypothesis of a synergic action between TrkB and CD20-Lyn pathways in dystrophic circulating $CD133^+$ stem cells after BDNF exposure, we decided to measure the intracellular free Ca^{2+} in normal and dystrophic circulating $CD133^+$ stem cells in unstimulated (basal) condition and after BDNF treatment. In normal circulating $CD133^+$ stem cells we found that BDNF was able to induce an increase in $[Ca^{2+}]_i$ that, even if appreciable, was not significant when compared to cells analyzed in basal condition ($p=0.122$). In contrast, calcium measurements performed on dystrophic circulating $CD133^+$ stem cells showed a significant increase between basal and BDNF treated cells ($p<0.001$). Moreover, observed intracellular Ca^{2+} increase was much higher in comparison to that obtained in normal circulating $CD133^+$ stem cells subjected to identical treatment. Data were collected from 2070 basal CTR, 2080 basal DMD, 2668 BDNF CTR and 2118 BDNF DMD cells. The differences marked by an asterisk are statistically significant ($p<0.001$ ANOVA).

more intense increase of $[Ca^{2+}]_i$ is thus expected. To assess this hypothesis, we performed experiments for the quantification of intracellular free Ca^{2+} in normal and dystrophic circulating $CD133^+$ stem cells in the unstimulated condition (basal) and after BDNF treatment. In normal circulating $CD133^+$ stem cells we found that BDNF was able to induce an increase in $[Ca^{2+}]_i$ that, even if appreciable, was not significant when compared to cells analyzed in basal condition ($p=0.122$) (Fig. 5 F). In contrast, calcium measurements performed on dystrophic circulating $CD133^+$ stem cells showed a significant increase between basal and BDNF treated cells ($p<0.001$) (Fig. 5 F). Moreover, the observed intracellular Ca^{2+} increase was much higher in comparison to that obtained in normal circulating $CD133^+$ stem cells subjected to identical treatment (Fig. 5 F). Data reported here describe a different response to BDNF in normal and dystrophic circulating $CD133^+$ stem cells in terms of intracellular calcium release, reflecting the fact that only in dystrophic circulating $CD133^+$ stem cells does the CD20-Lyn pathway undergo activation after BDNF exposure, leading to the supplementary calcium release observed.

Discussion

In this work we isolated circulating $CD133^+$ stem cells which possess myogenic potential [28] and first characterized their immunophenotype by FACS analysis. Unexpectedly, the results obtained by these experiments demonstrated the expression of the B-cell marker CD20 in normal and dystrophic circulating $CD133^+$ stem cells. The function of CD20 has not yet been fully elucidated, but evidence of its involvement in calcium homeostasis is growing. Initial work on CD20 signaling led to the hypothesis the CD20 might act as an ion channel to directly mediate cell signaling [39]. Experiments demonstrating increased calcium conductance in transfected cells expressing CD20 supports a role for CD20 in regulating intracellular Ca^{2+} [40]. More recently, siRNA experiments demonstrated reduced ion influx in B cells following reduced CD20 expression, potentially through a pathway involving the B-cell antigen receptor (BCR) and store-operated channels [41]. Together with these findings, supporting a direct role of CD20 in the regulation of transmembrane conductive Ca^{2+} flux, a CD20-related pathway able to act on intracellular Ca^{2+} level was also described. CD20 constitutively associates with lipid rafts, in which src-family kinases reside, and it was shown to be a component of a multimolecular complex that includes the tyrosine kinases Lyn, Fyn and Lck, and a 75/80 kD protein phosphorylated on tyrosine residues *in vivo* [36]. CD20-associated p75/80 has been identified as PAG, a ubiquitous, highly tyrosine-phosphorylated adaptor protein localized exclusively to lipid rafts [42, 43]. Also known as Csk-binding protein (Cbp), PAG recruits Csk to lipid rafts to maintain resident src-family tyrosine kinases in the inactive state. Changes in either the conformation of CD20 or its phosphorylation state, or both, could regulate its association with Lyn, Fyn and Lck, resulting in an activation of such kinases and initiating of downstream signaling [31, 36, 37]. The activation of Lyn, the src-kinase accounted for most of the PTK activity in the CD20 complex [36], triggers a cascade of events leading to Ca^{2+} mobilization from intracellular stores after activation of PLCγ2 and PI3-K [38]. Several observations suggest that an increase in $[Ca^{2+}]_i$ could be involved in the etiology of the Duchenne muscular dystrophy (DMD), a muscular disease due a deficiency in dystrophin protein [6–8, 10, 11]. Quantitative measurements of $[Ca^{2+}]_i$ showed a higher percentage of cells exceeding the reference value of 100 nM in the dystrophic circulating $CD133^+$ population than in the normal counterpart ($p<0.001$), giving evidence, for the first time, of an altered regulation of intracellular Ca^{2+} affecting dystrophic blood-derived $CD133^+$ stem cells. Moreover, we found a higher percentage of circulating $CD133^+CD20^+$ cells in DMD blood than the normal counterpart.

To elucidate the possible role of CD20 in the intracellular Ca^{2+} overload observed in dystrophic $CD133^+$ stem cells, we performed experiments to quantify the CD20 expression on the membrane of normal and dystrophic circulating $CD133^+$ stem cells and evaluate its phosphorylation state. While the number of CD20 molecules on the membrane of normal and DMD blood-derived $CD133^+$ stem cells was not significantly different, the high level of threonine phosphorylation observed in dystrophic circulating $CD133^+$ stem cells reflects a more consistent activation of the CD20-related downstream signaling pathway. These results support an involvement of CD20 in the Ca^{2+} impairment described in dystrophic circulating $CD133^+$ stem cells, related to an altered functionality of its signaling activity and not to the number of the CD20 molecules expressed on the dystrophic circulating $CD133^+$ stem cell membrane.

Based on the absence of physiological agonists able to bind and induce CD20 phosphorylation, we started to look for a soluble, released factor potentially able to promote, indirectly, CD20 activation. By ELISA analysis we demonstrated an abnormal BDNF release from the dystrophic circulating $CD133^+$ stem cells. For this reason, we focused our attention on the molecular pathways that undergo activation after interaction of

BDNF with its receptor TrkB. Presented results demonstrate a connection between BDNF/TrkB signaling and CD20 activation, since a strong induction of CD20 phosphorylation was observed both in normal and dystrophic circulating CD133$^+$ stem cells after BDNF treatment. The heavy threonine-phosphorylation observed in unstimulated DMD cells is, reasonably, a direct consequence of the higher BDNF release described above. Moreover, we show here that BDNF-induced phosphorylation of CD20 is not followed by the same intracellular events in normal and dystrophic blood-derived CD133$^+$ stem cells. Particularly, in both normal and dystrophic circulating CD133$^+$ stem cells we observed Lyn recruitment to CD20 after BDNF treatment. To the contrary, only in dystrophic circulating CD133$^+$ stem cells does the recruited src-kinase undergo phosphorylation, promoting the activation of additional intracellular pathways that can act in synergy with TrkB signaling in the modulation of intracellular Ca^{2+} levels. These data contribute to define a situation where the same stimulus (BDNF) results in a different response in normal and dystrophic blood-derived CD133$^+$ stem cells in term of an intracellular Ca^{2+} rise, according to the activation of different signaling pathways. In fact, while BDNF treatment of CD133$^+$ stem cells isolated from normal blood will result only in the activation of TrkB downstream signaling, in dystrophic blood-derived CD133$^+$ stem cells the synergic activation of TrkB and CD20-Lyn pathways will take place, leading to a supplemental intracellular free calcium increase. These considerations are strongly supported by measurements of intracellular free Ca^{2+} levels in BDNF stimulated normal and dystrophic circulating CD133$^+$ stem cells, revealing a more intense increase of $[Ca^{2+}]_i$ in dystrophic cells, as expected. Together, these data demonstrate that the intracellular Ca^{2+} overload observed in DMD blood-derived CD133$^+$ stem cells involved, at least, two factors acting in synergy: 1) an increased BDNF release, leading to an autocrine/paracrine activation of TrkB pathway; 2) the activation of CD20-Lyn signaling, resulting in a supplementary intracellular calcium increase. We speculate that the absence of dystrophin may affect the physiological integrity of the membrane of the DMD circulating CD133$^+$ stem cells, leading to an abnormal function of the CD20 membrane antigen. In this work we have demonstrated the expression of the Dp71 dystrophin isoform in normal blood-derived CD133$^+$ stem cells. Interestingly, we describe here the absence of Dp71 dystrophin isoform at protein level in dystrophic circulating CD133$^+$ stem cells.

Several works reported a reduced and/or compromised expression of Dp71, the ubiquitous dystrophin isoform, in dystrophic tissues that cannot be explained, at least formally, considering the site of mutation on the DMD gene. Altered Dp71 transcripts were found in astrocytes of patients with severe cerebral dysfunction [44] and an impaired oligomerization of Dp71 has been demonstrated in Dp427-deficient *mdx* brain [45]. Furthermore, a reduced expression of Dp71 was observed in endothelial and glial cells derived from *mdx* fetuses and in newborn and adult mice, associated with impaired blood-brain barrier (BBB) development [46]. Finally, Dp71 association with the cell membrane was demonstrated [47], identified in the platelet membrane cytoskeleton [48], and a critical role for the clustered localization of potassium channels in retinal glial cells was described [49].

All these data suggest that the absence of all dystrophin isoforms, included Dp71, in the DMD circulating CD133$^+$ stem cells, can lead to an impairment of the CD20-related signaling pathway, resulting in intracellular Ca^{2+} overload. However, further studies are needed to demonstrate the existence of a functional relationship between Dp71 and CD20, whether mediated by a CD20-Dp71 direct interaction or by an indirect link involving other dystrophin associated proteins.

The rescue of dystrophin expression in engineered dystrophic circulating CD133$^+$ stem cells provides the recovery of muscle force and endurance of dystrophic animal models after the transplantation of these cells [27]. Further experiments are needed to demonstrate that the correct expression of Dp71 dystrophin isoform on the engineered dystrophic circulating CD133$^+$ stem cells results in an intracellular Ca^{2+} normalization. The performance of additional research focused on the CD20-related signaling pathway will substantially enhance our understanding of the mechanism underlying the pathology of DMD and the behavior of dystrophic blood-derived CD133$^+$ stem cells and, in so doing, may lead to the improvement of strategies for the treatment of this disease.

Acknowledgements. This work has been supported by the Association Monégasque contre les Myopathies (AMM), the Duchenne Parent Project de France (DPP France), and the Associazione Amici del Centro Dino Ferrari. The authors have no conflicting financial interests.

1 Berridge, M. J., Lipp, P. and Bootman, M. D. (2000). The versatility and universality of calcium signalling. Nat. Rev. Mol. Cell Biol. 1, 11–21.
2 Carafoli, E. (2002). Calcium signaling: a tale for all seasons. Proc. Natl. Acad. Sci. U S A 99, 1115–22.
3 Clapham, D. E. (1995). Calcium signaling. Cell 80, 259–68.
4 Hoffman, E. P., Brown, R. H., Jr. and Kunkel, L. M. (1987). Dystrophin: the protein product of the Duchenne muscular dystrophy locus. Cell 51, 919–28.

5 Watkins, S. C., Hoffman, E. P., Slayter, H. S. and Kunkel, L. M. (1988). Immunoelectron microscopic localization of dystrophin in myofibres. Nature 333, 863–6.

6 Bertorini, T. E., Bhattacharya, S. K., Palmieri, G. M., Chesney, C. M., Pifer, D. and Baker, B. (1982). Muscle calcium and magnesium content in Duchenne muscular dystrophy. Neurology 32, 1088–92.

7 Bodensteiner, J. B. and Engel, A. G. (1978). Intracellular calcium accumulation in Duchenne dystrophy and other myopathies: a study of 567,000 muscle fibers in 114 biopsies. Neurology 28, 439–46.

8 Jackson, M. J., Jones, D. A. and Edwards, R. H. (1985). Measurements of calcium and other elements in muscle biopsy samples from patients with Duchenne muscular dystrophy. Clin. Chim. Acta 147, 215–21.

9 Bulfield, G., Siller, W. G., Wight, P. A. and Moore, K. J. (1984). X chromosome-linked muscular dystrophy (mdx) in the mouse. Proc. Natl. Acad. Sci. U S A 81, 1189–92.

10 Alderton, J. M. and Steinhardt, R. A. (2000). Calcium influx through calcium leak channels is responsible for the elevated levels of calcium-dependent proteolysis in dystrophic myotubes. J. Biol. Chem. 275, 9452–60.

11 Turner, P. R., Fong, P. Y., Denetclaw, W. F. and Steinhardt, R. A. (1991). Increased calcium influx in dystrophic muscle. J. Cell. Biol. 115, 1701–12.

12 Gillis, J. M. (1999). Understanding dystrophinopathies: an inventory of the structural and functional consequences of the absence of dystrophin in muscles of the mdx mouse. J. Muscle Res. Cell Motil. 20, 605–25.

13 Bakker, A. J., Head, S. I., Williams, D. A. and Stephenson, D. G. (1993). Ca2+ levels in myotubes grown from the skeletal muscle of dystrophic (mdx) and normal mice. J. Physiol. 460, 1–13.

14 Denetclaw, W. F., Jr., Hopf, F. W., Cox, G. A., Chamberlain, J. S. and Steinhardt, R. A. (1994). Myotubes from transgenic mdx mice expressing full-length dystrophin show normal calcium regulation. Mol. Biol. Cell 5, 1159–67.

15 Turner, P. R., Westwood, T., Regen, C. M. and Steinhardt, R. A. (1988). Increased protein degradation results from elevated free calcium levels found in muscle from mdx mice. Nature 335, 735–8.

16 Collet, C., Allard, B., Tourneur, Y. and Jacquemond, V. (1999). Intracellular calcium signals measured with indo-1 in isolated skeletal muscle fibres from control and mdx mice. J. Physiol. 520 Pt 2, 417–29.

17 Gailly, P., Boland, B., Himpens, B., Casteels, R. and Gillis, J. M. (1993). Critical evaluation of cytosolic calcium determination in resting muscle fibres from normal and dystrophic (mdx) mice. Cell Calcium 14, 473–83.

18 Head, S. I. (1993). Membrane potential, resting calcium and calcium transients in isolated muscle fibres from normal and dystrophic mice. J. Physiol. 469, 11–9.

19 Pressmar, J., Brinkmeier, H., Seewald, M. J., Naumann, T. and Rudel, R. (1994). Intracellular Ca2+ concentrations are not elevated in resting cultured muscle from Duchenne (DMD) patients and in MDX mouse muscle fibres. Pflugers Arch. 426, 499–505.

20 Constantin, B., Sebille, S. and Cognard, C. (2006). New insights in the regulation of calcium transfers by muscle dystrophin-based cytoskeleton: implications in DMD. J. Muscle Res. Cell Motil. 27, 375–86.

21 Rivet-Bastide, M., Imbert, N., Cognard, C., Duport, G., Rideau, Y. and Raymond, G. (1993). Changes in cytosolic resting ionized calcium level and in calcium transients during in vitro development of normal and Duchenne muscular dystrophy cultured skeletal muscle measured by laser cytofluorimetry using indo-1. Cell Calcium 14, 563–71.

22 Imbert, N., Cognard, C., Duport, G., Guillou, C. and Raymond, G. (1995). Abnormal calcium homeostasis in Duchenne muscular dystrophy myotubes contracting in vitro. Cell Calcium 18, 177–86.

23 Vandebrouck, C., Martin, D., Colson-Van Schoor, M., Debaix, H. and Gailly, P. (2002). Involvement of TRPC in the abnormal calcium influx observed in dystrophic (mdx) mouse skeletal muscle fibers. J. Cell. Biol. 158, 1089–96.

24 Deval, E., Levitsky, D. O., Marchand, E., Cantereau, A., Raymond, G. and Cognard, C. (2002). Na(+)/Ca(2+) exchange in human myotubes: intracellular calcium rises in response to external sodium depletion are enhanced in DMD. Neuromuscul. Disord. 12, 665–73.

25 Liberona, J. L., Powell, J. A., Shenoi, S., Petherbridge, L., Caviedes, R. and Jaimovich, E. (1998). Differences in both inositol 1,4,5-trisphosphate mass and inositol 1,4,5-trisphosphate receptors between normal and dystrophic skeletal muscle cell lines. Muscle Nerve 21, 902–9.

26 Marchand, E., Constantin, B., Balghi, H., Claudepierre, M. C., Cantereau, A., Magaud, C., Mouzou, A., Raymond, G., Braun, S. and Cognard, C. (2004). Improvement of calcium handling and changes in calcium-release properties after mini- or full-length dystrophin forced expression in cultured skeletal myotubes. Exp. Cell Res. 297, 363–79.

27 Benchaouir, R., Meregalli, M., Farini, A., D'Antona, G., Belicchi, M., Goyenvalle, A., Battistelli, M., Bresolin, N., Bottinelli, R., Garcia, L. and Torrente, Y. (2007). Restoration of human dystrophin following transplantation of exon-skipping-engineered DMD patient stem cells into dystrophic mice. Cell Stem Cell 1, 646–57.

28 Torrente, Y., Belicchi, M., Sampaolesi, M., Pisati, F., Meregalli, M., D'Antona, G., Tonlorenzi, R., Porretti, L., Gavina, M., Mamchaoui, K., Pellegrino, M. A., Furling, D., Mouly, V., Butler-Browne, G. S., Bottinelli, R., Cossu, G. and Bresolin, N. (2004). Human circulating AC133(+) stem cells restore dystrophin expression and ameliorate function in dystrophic skeletal muscle. J. Clin. Invest. 114, 182–95.

29 Lowry, O. H., Rosebrough, N. J., Farr, A. L. and Randall, R. J. (1951). Protein measurement with the Folin phenol reagent. J. Biol. Chem. 193, 265–75.

30 Grynkiewicz, G., Poenie, M. and Tsien, R. Y. (1985). A new generation of Ca2+ indicators with greatly improved fluorescence properties. J. Biol. Chem. 260, 3440–50.

31 Deans, J. P., Li, H. and Polyak, M. J. (2002). CD20-mediated apoptosis: signalling through lipid rafts. Immunology 107, 176–82.

32 Genot, E. M., Meier, K. E., Licciardi, K. A., Ahn, N. G., Uittenbogaart, C. H., Wietzerbin, J., Clark, E. A. and Valentine, M. A. (1993). Phosphorylation of CD20 in cells from a hairy cell leukemia cell line. Evidence for involvement of calcium/calmodulin-dependent protein kinase II. J. Immunol. 151, 71–82.

33 Tedder, T. F., McIntyre, G. and Schlossman, S. F. (1988). Heterogeneity in the B1 (CD20) cell surface molecule expressed by human B-lymphocytes. Mol. Immunol. 25, 1321–30.

34 Valentine, M. A., Licciardi, K. A., Clark, E. A., Krebs, E. G. and Meier, K. E. (1993). Insulin regulates serine/threonine phosphorylation in activated human B lymphocytes. J. Immunol. 150, 96–105.

35 Valentine, M. A., Meier, K. E., Rossie, S. and Clark, E. A. (1989). Phosphorylation of the CD20 phosphoprotein in resting B lymphocytes. Regulation by protein kinase C. J. Biol. Chem. 264, 11282–7.

36 Deans, J. P., Kalt, L., Ledbetter, J. A., Schieven, G. L., Bolen, J. B. and Johnson, P. (1995). Association of 75/80-kDa phosphoproteins and the tyrosine kinases Lyn, Fyn, and Lck with the B cell molecule CD20. Evidence against involvement of the cytoplasmic regions of CD20. J. Biol. Chem. 270, 22632–8.

37 Deans, J. P., Schieven, G. L., Shu, G. L., Valentine, M. A., Gilliland, L. A., Aruffo, A., Clark, E. A. and Ledbetter, J. A. (1993). Association of tyrosine and serine kinases with the B cell surface antigen CD20. Induction via CD20 of tyrosine phosphorylation and activation of phospholipase C-gamma 1 and PLC phospholipase C-gamma 2. J. Immunol. 151, 4494–504.

38 Yamanashi, Y., Fukui, Y., Wongsasant, B., Kinoshita, Y., Ichimori, Y., Toyoshima, K. and Yamamoto, T. (1992). Activation of Src-like protein-tyrosine kinase Lyn and its association with phosphatidylinositol 3-kinase upon B-cell antigen receptor-mediated signaling. Proc. Natl. Acad. Sci. U S A 89, 1118–22.
39 Einfeld, D. A., Brown, J. P., Valentine, M. A., Clark, E. A. and Ledbetter, J. A. (1988). Molecular cloning of the human B cell CD20 receptor predicts a hydrophobic protein with multiple transmembrane domains. Embo J. 7, 711–7.
40 Bubien, J. K., Zhou, L. J., Bell, P. D., Frizzell, R. A. and Tedder, T. F. (1993). Transfection of the CD20 cell surface molecule into ectopic cell types generates a Ca2+ conductance found constitutively in B lymphocytes. J. Cell. Biol. 121, 1121–32.
41 Li, H., Ayer, L. M., Lytton, J. and Deans, J. P. (2003). Store-operated cation entry mediated by CD20 in membrane rafts. J. Biol. Chem. 278, 42427–34.
42 Brdicka, T., Pavlistova, D., Leo, A., Bruyns, E., Korinek, V., Angelisova, P., Scherer, J., Shevchenko, A., Hilgert, I., Cerny, J., Drbal, K., Kuramitsu, Y., Kornacker, B., Horejsi, V. and Schraven, B. (2000). Phosphoprotein associated with glycosphingolipid-enriched microdomains (PAG), a novel ubiquitously expressed transmembrane adaptor protein, binds the protein tyrosine kinase csk and is involved in regulation of T cell activation. J. Exp. Med. 191, 1591–604.
43 Kawabuchi, M., Satomi, Y., Takao, T., Shimonishi, Y., Nada, S., Nagai, K., Tarakhovsky, A. and Okada, M. (2000). Transmembrane phosphoprotein Cbp regulates the activities of Src-family tyrosine kinases. Nature 404, 999–1003.
44 Moizard, M. P., Billard, C., Toutain, A., Berret, F., Marmin, N. and Moraine, C. (1998). Are Dp71 and Dp140 brain dystrophin isoforms related to cognitive impairment in Duchenne muscular dystrophy? Am. J. Med. Genet. 80, 32–41.
45 Culligan, K., Glover, L., Dowling, P. and Ohlendieck, K. (2001). Brain dystrophin-glycoprotein complex: persistent expression of beta-dystroglycan, impaired oligomerization of Dp71 and up-regulation of utrophins in animal models of muscular dystrophy. BMC Cell Biol. 2, 2.
46 Nico, B., Paola Nicchia, G., Frigeri, A., Corsi, P., Mangieri, D., Ribatti, D., Svelto, M. and Roncali, L. (2004). Altered blood-brain barrier development in dystrophic MDX mice. Neuroscience 125, 921–35.
47 Rapaport, D., Greenberg, D. S., Tal, M., Yaffe, D. and Nudel, U. (1993). Dp71, the nonmuscle product of the Duchenne muscular dystrophy gene is associated with the cell membrane. FEBS Lett. 328, 197–202.
48 Austin, R. C., Fox, J. E., Werstuck, G. H., Stafford, A. R., Bulman, D. E., Dally, G. Y., Ackerley, C. A., Weitz, J. I. and Ray, P. N. (2002). Identification of Dp71 isoforms in the platelet membrane cytoskeleton. Potential role in thrombin-mediated platelet adhesion. J. Biol. Chem. 277, 47106–13.
49 Connors, N. C. and Kofuji, P. (2002). Dystrophin Dp71 is critical for the clustered localization of potassium channels in retinal glial cells. J. Neurosci. 22, 4321–7.

To access this journal online:
http://www.birkhauser.ch/CMLS